Exploring Optoelectronic Properties of Ultrawide Bandgap Semiconductors and Deep-Ultraviolet Spectroscopy

ISHII Ryota

Ultrawide bandgap (UWBG) semiconductors have attracted much attention for deep-ultraviolet (DUV) photonics and high-power electronics. However, the physical understanding is in infancy, preventing the potential capacities of UWBG semiconductors to be drawn out. The electronic and optical properties should be fully elucidated using such as DUV spectroscopy. However, one problem stands that DUV spectroscopy itself is immature. Therefore, we have been exploring both DUV spectroscopy and optoelectronic properties of UWBG semiconductors. Herein, we introduce the development of a deep-ultraviolet scanning near-field optical microscope operating at world's shortest wavelength, and discovery of feasible *p*-type electric conductivity control by Mg doping in AlN using deep-ultraviolet spectroscopy.

Introduction

Figure 1 shows the relationship between the lattice constant and bandgap (energy gap) in various semiconductors. In the early days of semiconductor research, materials with a small bandgap, such as Ge, Si, and GaAs, were main research targets. Today, thanks to the basic research on these materials, semiconductor industries have grown into a huge market, and semiconductor electronics has become an indispensable part of our modern society. From around 1970s, basic research on so-called "wide bandgap semiconductors", such as SiC and GaN, began. Owing to the tireless efforts by researchers and engineers, low-loss/high-voltage power devices and high-efficiency white LEDs have been realized. These applications utilizing wide bandgap semiconductors support today's and future energy-saving societies.

Currently, semiconducting materials with even wider bandgap, "ultrawide bandgap (UWBG) semiconductors" are attracting much attention as next-generation materials.

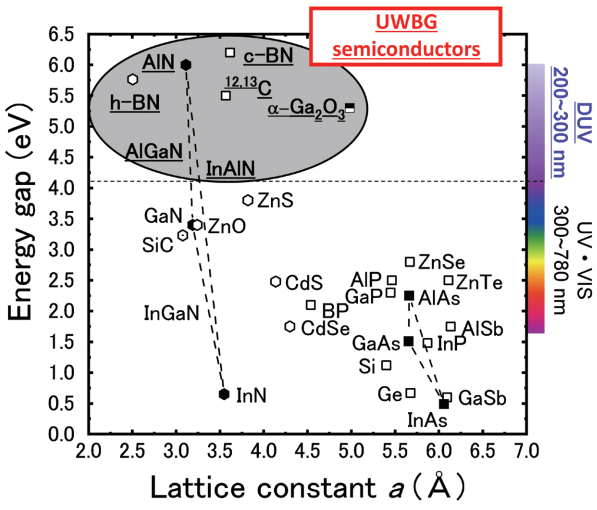

Figure 1 Lattice constant vs energy gap. (Deep-ultraviolet (DUV) ray: 200~300 nm).

As shown in Figure 1, from the viewpoint of optical devices, deep-ultraviolet (DUV) light-emitting devices can be fabricated using UWBG semiconductors. From the viewpoint of electronic devices, ultrahigh voltage power devices can be realized. Notably, DUV light-emitting devices are capable of inactivating influenza- and coronaviruses, and purifying water (900 million people on earth cannot drink clean water). Therefore, DUV light-emitting devices using UWBG semiconductors are expected to dramatically improve the world's sanitary environment.

However, the external quantum efficiency of DUV LEDs using UWBG semiconductors is currently low (Figure 2). The reasons should originate from such as the immaturity of the bulk crystal growth, epitaxial growth, and device processing technologies. In addition, our group focuses on the lack of the understanding of the optoelectronic properties of UWBG semiconductors such as aluminum nitride (AlN) and diamond.

To draw out the potential capacities of UWBG semiconductors, the electronic and optical properties should be fully elucidated using such as DUV spectroscopy. However, one problem arises that DUV spectroscopy itself is immature[1]. Therefore, we have been studying DUV spectroscopy and optoelectronic properties of UWBG semiconductors. These include the development of a DUV scanning near-field optical microscope (SNOM)[2], intrinsic exciton physics[3] and donor/acceptor impurity physics in AlN[4], recombination processes in AlGaN DUV LEDs[5], and isotopic effects on excitons in diamond[6]. In this manuscript, we will introduce some of our recent works[2,4].

Development of a deep-ultraviolet scanning near-field optical microscope (DUV SNOM)

Classical optics tells that the lateral resolution R is determined by $R=k_1$ (λ/NA), where k_1 is the experimental factor, λ is the optical wavelength, and NA is the numerical aperture[7]. Therefore, the lateral resolution of lithography has been enhanced by shortening the wavelength of light sources. The immersion argon-fluoride technique (λ=193 nm) has achieved R as small as 40 nm[8]. On the other hand, the lateral resolution of DUV luminescence (fluorescence) spectroscopy is limited at R>300 nm[9]. This relatively large value stems from the fact that luminescence spectroscopy requires wider spectral bandwidths. In the DUV spectral region, it is very difficult to design an objective lens with a high NA and broadband chromatic-aberration correction[1].

One approach to resolve the issue is luminescence spectroscopy using a SNOM which can overcome the diffraction limit of light[10,11]. Table 1 summarizes the development history of DUV SNOM in literature. The previous DUV SNOM cannot investigate luminescence signals below λ=240 nm due to the constraints. Therefore, we developed a DUV SNOM with an excitation wavelength of 210 nm to overcome the problem. Because of the immaturity of DUV spectroscopy, we designed and built a DUV SNOM from scratch: excitation optical system, objective optical system, scanning probe system, illumination optical system, imaging optical system, and detection optical system.

We used a fourth harmonic generation of a continuous-wave (CW) Ti:sapphire laser as an excitation source. The wavelength was adjusted to 210 nm. Unlike pulsed lasers, CW lasers realized luminescence measurements with a high signal-to-noise ratio. A serious problem in DUV spectroscopy was the temporal deterioration of transmission and reflection optics, which caused the power and pointing instability of the excitation beam. To solve the issue, we constructed a power and pointing stabilizing optical systems composed of two negative-feedback control.

The objective optical system consisted of a custom dichroic mirror and a reflective objective. The reflective

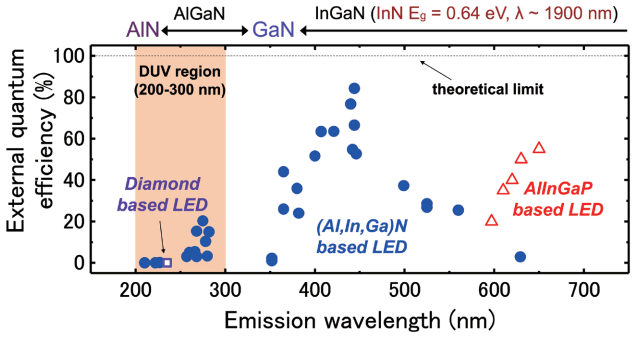

Figure 2 Current status of ultraviolet and visible LEDs.

Table 1 Development history of DUV SNOM (I: illumination, C: collection, PL:photoluminescence,EL: electroluminescence)

References	Excitation λ (nm)	Configuration	R (nm)	Experiment, samples
Sands *et al.*, J. Raman. Spectrosc. **33**, 730 (2002).	244	I mode	200	Raman signals, diamond
Aoki *et al.*, APL **84**, 356 (2004).	266	I mode	50	PL signals, organic materials
Taguchi *et al.*, J. Raman. Spectrosc. **40**, 1324 (2009).	266	I mode	30	Raman signals, diamond
Pinos *et al.*, APL **95**, 181914 (2009).	285	C mode	150	EL signals, AlGaN LED
Pinos *et al.*, JAP **109**, 113516 (2011).	258	I-C mode	100	PL signals, $Al_{0.3\sim0.5}GaN$ layers
Marcinkevičius *et al.*, APL **105**, 241108 (2014).	227	I-C mode	100	PL signals, $Al_{0.6\sim0.7}GaN$ layers

objective did not introduce chromatic aberrations which were ones of the most serial problems in DUV spectroscopy. Compared to a conventional SNOM used in the visible and near-infrared spectral regions, we used a short (3 mm) double-tapered[12] optical fiber probe to ensure a high-throughput transmission of DUV light. The distance between the optical fiber probe and the sample surface was controlled by the shear-force method[13].

The illumination optical system consisted of an incandescent lamp and a liquid light guide with a large core diameter. The beam was collimated by a visible achromatic lens and focused onto an optical fiber probe by a reflective objective. Thanks to the liquid light guide, the image of the optical fiber probe was clearly projected despite the critical illumination optical design.

A DUV imaging lens with a focal length of 105 mm was used in an imaging optical system. The magnification ratio of the imaging optical system was 5.4. The optical fiber probe and sample were imaged by a charged-coupled device camera with UV sensitivity.

The detection optical system consisted of a custom long pass filter and an apochromatic lens with a focal length of 50 mm. The chromatic aberration of this refractive lens was corrected from the DUV to the near-infrared spectral region. The luminescence signals were focused onto the entrance slit of a monochromator, dispersed by a grating, and then electrically detected by a liquid-nitrogen cooled charge coupled device. The whole experimental setup is detailed elsewhere[2].

Figure 3(a) shows the spectrally integrated photoluminescence (PL) intensity mapping images of an $Al_{0.8}Ga_{0.2}N$/AlN single quantum well structure taken by our DUV SNOM. The strong emission inhomogeneity was observed, which was consistent with the previous cathodoluminescence study[14]. The estimated lateral resolution from Figure 3(a) was better than 150 nm. Figure 3(b) shows the SNOM-PL spectra of the same sample at room temperature, demonstrating that our DUV-SNOM can detect luminescence signals below λ=240 nm with an excitation wavelength of 210 nm. In conclusion, we developed a DUV SNOM for luminescence spectroscopy which can operate at the shortest wavelength in the world.

P-type electric conductivity control of AlN

Bipolar (*n*- and *p*-type) electric conductivity control is at the heart of semiconductor technologies and has been a major challenge in UWBG semiconductors because of the very high donor and/or acceptor binding energies. In the case of AlN, the *p*-type electric conductivity control by Mg doping is believed to be unfeasible. We casted a doubt on the consensus and experimentally and theoretically revisited the substitutional Mg acceptor binding energy of AlN by means of DUV spectroscopy[4].

Bound exciton PL spectroscopy was conducted using a pulsed ArF excimer laser with an excitation wavelength of 193 nm. The PL signals were dispersed by a 50-cm monochromator and detected by a liquid-nitrogen-cooled charge-coupled device. The spectral resolution was better than 0.7 meV.

Figure 4 shows the PL spectra of unintentionally doped (UID), Si-doped (Si#1), and Mg-doped (Mg#1, Mg#2, and Mg#3) AlN samples at 11 K. The 6.0262 eV (denoted as Γ_5) and 6.039 eV (denoted as Γ_1^L) peaks were assigned to free exciton (intrinsic) emissions, as can be understood from the fact that nearly the same emissions are observed irrespective to Si and Mg doping. On the contrary, the 6.0110 eV peak (denoted as Si^0X) is strongly observed for Si-doped AlN, indicating that the origin is extrinsic (assigned to a neutral Si donor bound exciton). We herein

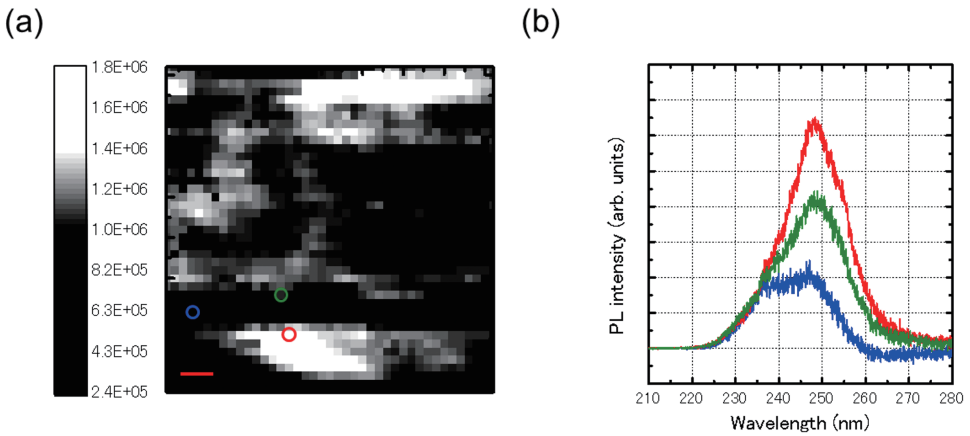

Figure 3 (a) Spectrally integrated PL intensity mapping images (2 μm × 2 μm) of an $Al_{0.8}Ga_{0.2}N$/AlN single quantum well structure. The red bar denotes 200 nm. (b) The SNOM-PL spectra at room temperature. The color of spectra corresponds to the positions in Figure 3(a).

assigned the 6.0030 eV to a neutral Mg acceptor bound exciton transition (denoted as Mg^0X). The energy difference between the neutral Mg acceptor bound exciton transition and the lowest free exciton transition (Γ_5) was 23.2 meV. Using a well-known empirical rule called Haynes' rule, we tentatively estimated the Mg acceptor binding energy of AlN to 258-390 meV.

We also performed the impurity-related transition luminescence spectroscopy and acceptor-binding-energy calculation using variational methods. The detail is written elsewhere[4]. Our three independent approaches estimated the substitutional Mg acceptor binding energy of AlN to be 330±80 meV which was substantially smaller than the commonly accepted value of at least 500 meV.

Figure 5 summarizes the relation between the room-temperature bandgap and substitutional donor/acceptor binding energies of wide and ultrawide bandgap semiconductors. Because the high *p*-type electric conductivity has been achieved in diamond by boron doping whose acceptor binding energy is 370 meV, our estimated Mg acceptor binding energy of AlN suggested that the *p*-type electric conductivity control by Mg doping is feasible in AlN.

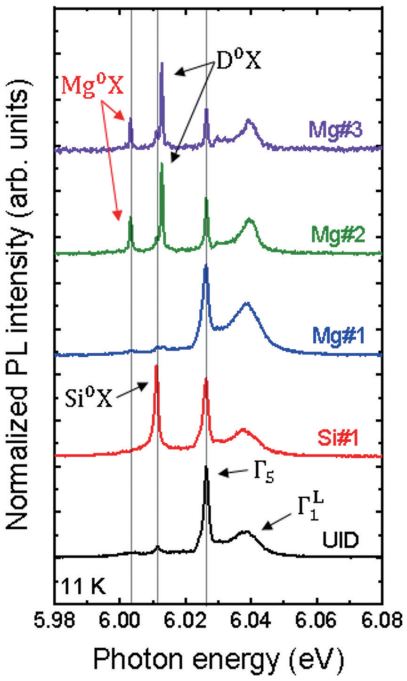

Figure 4 PL spectra of UID, Si-doped, and Mg-doped AlN samples at 11 K.

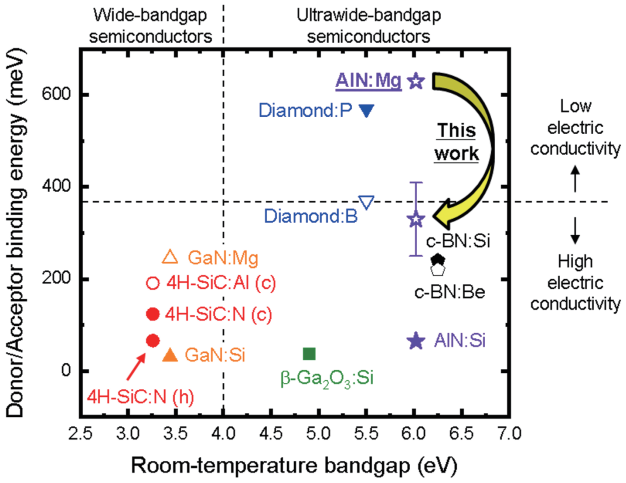

Figure 5 Relation between the room-temperature bandgap and substitutional donor/acceptor binding energies of select wide and ultrawide bandgap semiconductors.

Conclusion

We briefly introduced two of our recent works, the development of a DUV SNOM operating at world's shortest wavelength, and discovery of feasible *p*-type electric conductivity control by Mg doping in AlN using DUV luminescence spectroscopy. We will continue to explore the optoelectronic properties of UWBG semiconductors and DUV spectroscopy to make our future better.

References

[1] Y. Ozaki and S. Kawata, *"Far- and Deep-Ultraviolet spectroscopy"* (Springer, Japan, 2015).
[2] R. Ishii *et al., APL Photon*. 4, 070801 (2019).
[3] R. Ishii *et al., Phys. Rev. B* 87, 161204R (2013), *Phys. Rev. B* 102, 155202 (2020).
[4] R. Ishii *et al., Jpn. J. Appl. Phys*. 60, 080901 (2021), *Phys. Rev. B* 108, 035205 (2023).
[5] R. Ishii *et al., Appl. Phys. Express.* 13, 102005 (2020), *AIP Adv.* 10, 125014 (2020).
[6] R. Ishii *et al., Jpn. J. Appl. Phys.* 58, 010904 (2019), *Jpn. J. Appl. Phys.* 59, 010903 (2020).
[7] T. Ito and S. Okazaki, *Nature* 406, 1027 (2007).
[8] M. Totzeck, W. Ulrich, A. Göhnermeier, and W. Kaiser, *Nat. Photonics* 1, 629 (2007).
[9] F. Jamme, S. Villette, A. Giuliani, V. Rouam, F. Wien, B. Lagarde, S. Kascakova, S. Villette, F. Allouche, S. Pallu, V. Rouam, and M. Réfrégiers, *Microsc. Microanal.* 16, 507 (2010).
[10] D. W. Pohl, W. Denk, and M. Lanz, *Appl. Phys. Lett.* 44, 651 (1984).
[11] E. Betzig and J. K. Trautman, *Science* 257, 189 (1992).
[12] T. Saiki and K. Matsuda, *Appl. Phys. Lett*. 74, 2773 (1999).
[13] E. Betzig, P. L. Finn, and J. S. Weiner, *Appl. Phys. Lett*. 60, 2484 (1992).
[14] M. Funato, R. G. Banal, and Y. Kawakami, *AIP Adv*. 5, 117115 (2015).

Dr. ISHII Ryota

Assistant Professor,
Department of electronic Science and Engineering,
Kyoto University